THE JOURNAL OF PHYSICAL CHEMISTRY Letters

Letter

pubs.acs.org/JPCL

Transition-Path Probability as a Test of Reaction-Coordinate Quality Reveals DNA Hairpin Folding Is a One-Dimensional Diffusive Process

Krishna Neupane,[†] Ajay P. Manuel,[†] John Lambert,[†] and Michael T. Woodside*[,†,‡]

[†]Department of Physics, University of Alberta, 4-181 CCIS, Edmonton, Alberta T6G 2E1, Canada

[‡]National Institute for Nanotechnology, National Research Council Canada, 11421 Saskatchewan Drive, Edmonton, Alberta T6G 2M9, Canada

Supporting Information

ABSTRACT: Chemical reactions are typically described in terms of progress along a reaction coordinate. However, the quality of reaction coordinates for describing reaction dynamics is seldom tested experimentally. We applied a framework for gauging reaction-coordinate quality based on transition-path analysis to experimental data for the first time, looking at folding trajectories of single DNA hairpin molecules measured under tension applied by optical tweezers. The conditional probability for being on a reactive transition path was compared with the probability expected for ideal diffusion over a 1D energy landscape based on the committor function. Analyzing measurements and simulations of hairpin folding where end-to-end extension is the reaction coordinate, after accounting for instrumental effects on the analysis, we found good agreement between transition-path and committor analyses for model two-state hairpins, demonstrating that folding is well-described by 1D diffusion. This work establishes transition-path analysis as a powerful new tool for testing experimental reaction-coordinate quality.

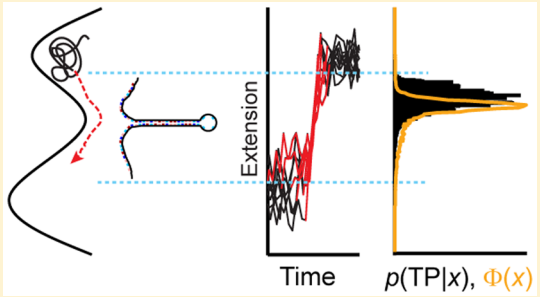

INTRODUCTION

The molecular mechanisms of chemical reactions as varied as bond formation, ligand binding, conformational change, and biopolymer folding are typically conceived in terms of passage through a transition state separating the reactants and products.[1,2] The coordinate along which the progress of the reaction is measured is known as the reaction coordinate. Ideally, reaction coordinates should capture the essential dynamics occurring during a reaction. However, when the multiple degrees of freedom typical of most reactions are projected onto a single coordinate, such as a convenient experimental observable, the nature of this projection affects the ability to describe the dynamics along that coordinate. "Good" coordinates faithfully reflect the full dynamics of the reaction and allow the likely outcome of a trajectory to be predicted, whereas "bad" coordinates can result in non-Markovian dynamics, where memory effects degrade predictive ability.[3−5] Whereas it is possible to optimize the choice of reaction coordinate used in computational studies,[6,7] in experiments the reaction coordinate is typically imposed by the choice of assay used. It is thus essential to be able to assess the quality of experimental reaction coordinates.

The issue of reaction-coordinate quality is particularly acute for studies of structure formation ("folding") in biological molecules like proteins and nucleic acids. Folding is typically described in terms of a diffusive search for the minimum-energy structure in a multidimensional landscape representing the energy of the molecule as a function of all possible conformations.[8−10] Experimentally, monitoring the folding transition along an observable reaction coordinate thus projects the full landscape, with hundreds or thousands of degrees of freedom, onto a single dimension. Although such projections represent a gross approximation, 1D descriptions of folding are widely used, being conveniently simple to implement, and they often appear to be quite successful.[10−19] However, the quality of the reaction coordinate is rarely tested, even though it can have critical implications for interpreting experimental results, and poor reaction coordinates may lead to incorrect conclusions.[20−22]

A test of reaction-coordinate quality that was developed specifically for folding reactions is the splitting probability or committor, $p_{fold}(x)$—the probability that when the molecule starts at position x on the reaction coordinate it will reach the folded state before the unfolded state.[23] For a transition involving two states separated by a single barrier (Figure 1A, black), $p_{fold}(x)$ should be roughly 0 in the unfolded potential well, 1 in the folded well, and 1/2 at the top of the barrier. Committor analysis has been applied in computational studies[24,25] but rarely in experimental work. Two notable examples involved folding trajectories of single molecules held under tension by a force probe (e.g., atomic force microscope or laser tweezers, Figure 1B), where the molecular extension was measured as the reaction coordinate. Such measurements are well-suited for judging reaction-coordinate quality because

Received: January 26, 2015
Accepted: March 4, 2015
Published: March 4, 2015

DOI: 10.1021/acs.jpclett.5b00176
J. Phys. Chem. Lett. 2015, 6, 1005−1010

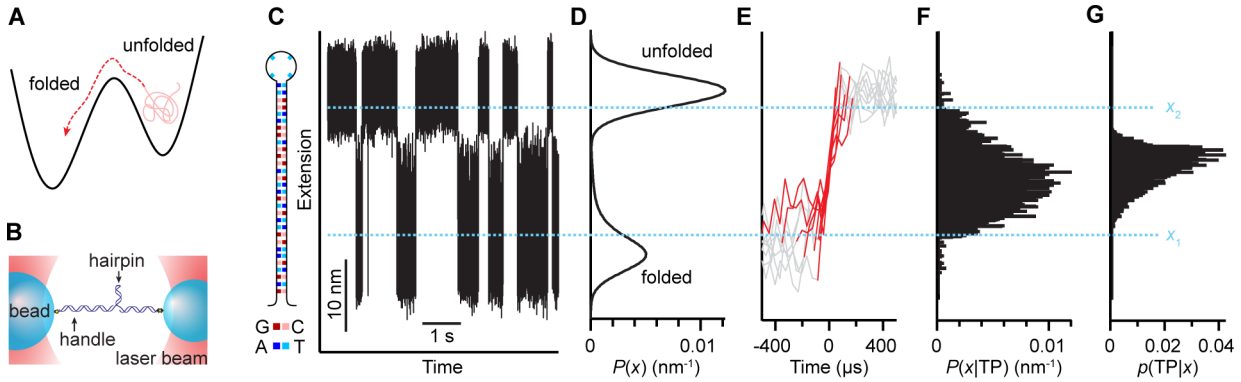

Figure 1. Transition-path analysis of DNA hairpin trajectory under constant force. (A) Schematic of thermally activated escape over an energy barrier, as in folding, indicating the transition path (red) as the portion of the trajectory that crosses the barrier. (B) Schematic of force spectroscopy measurement: a single DNA hairpin is attached to double-stranded DNA handles bound to beads held in optical traps. (C) Portion of a constant-force trajectory of the molecular extension of the hairpin construct. Inset: sequence of hairpin 30R50/T4. (D) Equilibrium distribution of extension values shows two peaks, corresponding to folded and unfolded states. (E) Set of unfolding transition paths (red) passing between x_1 and x_2 (dotted lines), taken from the full extension trajectory. (F) Distribution of molecular extension along the transition paths. (G) Conditional probability of being on a transition path at a given extension is highly peaked but has much smaller amplitude than expected.

the rare reactive transitions can be readily identified from among the majority of nonproductive conformational fluctuations. Using a tensegrity parameter to check whether $p_{fold} = 1/2$ at the barrier between the two states,[26] extension was judged to be a reasonable reaction coordinate for optical tweezers measurements of several DNA hairpins[27] and one of the folding transitions in the GCN4 leucine zipper.[28] In contrast, a comparison of $p_{fold}(x)$ calculated directly from the trajectory of one of the same DNA hairpins, as opposed to calculated from the potential of mean force (PMF) implied by the equilibrium extension distribution, disagreed with this conclusion, suggesting that extension was not such a good coordinate.[29]

Tests such as these based on p_{fold} provide important insight into the reaction coordinate but suffer from notable limitations. For example, while the requirement that $p_{fold} = 1/2$ at the barrier is simple to apply, it represents a minimal criterion for a good reaction coordinate: necessary but perhaps not sufficient. Comparing trajectory- and landscape-derived $p_{fold}(x)$ curves requires either assuming that the diffusion coefficient D along the reaction coordinate is constant—an assumption often made for simplicity but generally incorrect[7,14,30,31]—or else knowing the position-dependent values of $D(x)$ along the entire reaction coordinate,[29] something that is very challenging to determine experimentally.

An alternate approach that avoids these issues was proposed based on the statistics of the transition paths, the fleeting parts of the trajectory where the molecule actually crosses over the barrier and switches between states (Figure 1a, red). The conditional probability that the molecule is on a transition path when it has extension x, $p(\mathrm{TP}|x)$, should be highly peaked around the location of the barrier, $x^{\ddagger}$, ideally reaching a peak of 1/2 at $x^{\ddagger}$.[32] $p(\mathrm{TP}|x)$ can be calculated from a folding trajectory in equilibrium using a Bayesian relation between the equilibrium and transition-path ensembles[6,32]

$$p(\mathrm{TP}|x) = P(x|\mathrm{TP})p(\mathrm{TP})/P(x) \quad (1)$$

where $P(x)$ is the equilibrium distribution of extension values in the complete trajectory, $P(x|\mathrm{TP})$ is the distribution of extension values along only the transition paths (i.e., excluding all nonproductive fluctuations), and $p(\mathrm{TP})$ is the fraction of time in the trajectory spent on transition paths. For pure 1D diffusion, one expects[6] $p(\mathrm{TP}|x) = 2p_{fold}(x)[1 - p_{fold}(x)]$.

Transition-path analysis has been applied to computational simulations and models of chemical reactions and protein folding[6,16] but not yet directly to experimental data. Here we apply it to folding reactions, investigating the quality of molecular extension as a reaction coordinate in single-molecule force spectroscopy (SMFS) measurements. SMFS has been widely applied to folding phenomena over the last two decades, providing exciting insight into the folding of nucleic acids[33] and proteins[34] and a powerful way to probe folding landscapes.[35] However, the quality of molecular extension as a reaction coordinate has been tested only sparsely,[26,29] even though important questions have arisen in recent years about how to interpret such measurements.[21,35]

We first applied transition-path analysis to folding trajectories of the two-state DNA hairpin 30R50/T4[36] (Figure 1C, inset), attached to kilobase-long handles of double-stranded DNA bound specifically to polystyrene beads held by dual-trap optical tweezers (Figure 1B) under constant force.[37] The trajectory of the end-to-end extension (Figure 1C) was binned to generate the equilibrium distribution $P(x)$ (Figure 1D), revealing two peaks corresponding to folded and unfolded states at low and high extension values, respectively. The transition paths (Figure 1E, red) were identified as those parts of the trajectory crossing between the boundaries x_1 and x_2 (Figure 1C, dotted lines), located between the folded and unfolded states but bracketing the majority of the distance between them. The extension values measured along the transition paths were pooled for all such paths to generate the transition-path distribution $P(x|\mathrm{TP})$ (Figure 1F); $p(\mathrm{TP}|x)$ was then calculated from eq 1 (Figure 1g). (For details of experiments and analysis, see Supporting Information (SI).)

The result looks only partially successful: Although $p(\mathrm{TP}|x)$ is fairly sharply peaked, with a width of 20−25% of the total distance between folded and unfolded states, it peaks at only 0.04, much lower than expected. Naively, this result suggests that extension is a poor reaction coordinate for this molecule. However, this analysis does not take into account the potential effects of additional noise in the data beyond the fluctuations expected from diffusive motion of the hairpin over its intrinsic landscape, such as the extra fluctuations that arise from Brownian motion of the compliant dumbbell (DNA tethers and beads) used experimentally to probe the hairpin.

DOI: 10.1021/acs.jpclett.5b00176
J. Phys. Chem. Lett. 2015, 6, 1005−1010

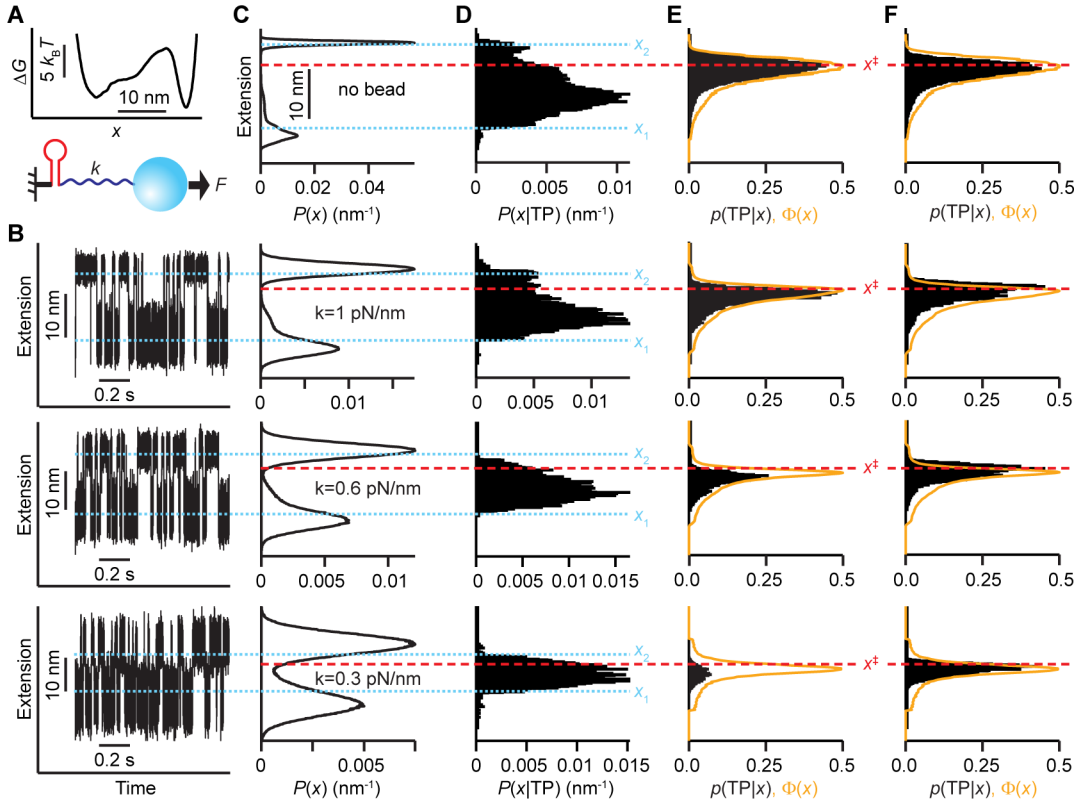

Figure 2. Simulations of effect of instrumental compliance on transition-path analysis. (A) Schematic of simulation: molecule tethered to a bead experiencing a constant force via a compliant tether with stiffness k. Inset: folding landscape in simulation. (B) Simulated extension trajectories at different k (top to bottom: 1, 0.6, and 0.3 pN/nm). (C) Equilibrium extension distributions show increasing broadening of the folded- and unfolded-state peaks with increasing compliance (top to bottom: no bead/tether, k = 1, 0.6, and 0.3 pN/nm). Dotted lines: boundaries defining transition paths. Dashed line: barrier location. (D) Extension distributions along the transition paths are similar for all simulations. (E) $p(\mathrm{TP}|x)$ (black) is highly peaked near $x^‡$ (dashed line) in all cases, but the peak amplitude decreases with increasing tether compliance. $p(\mathrm{TP}|x)$ agrees well with $\Phi(x)$ (orange) expected from the committor in the high-stiffness and no-tether cases but does not agree well for more compliant tethers. (F) $p(\mathrm{TP}|x)$ (black) agrees well with $\Phi(x)$ (orange) in all cases after correcting for the effects of tether compliance.

To explore how such instrumental effects alter the result, we simulated a constant-force trajectory of a molecule tethered compliantly to a bead subjected to a constant force (Figure 2A), mimicking the experiment as previously described.[38] In this simulation, the folding involves purely 1D diffusion over the landscape illustrated in Figure 2A (inset). The reaction coordinate is thus by definition "good," and the effects of changing instrumental parameters can be explored without experimental complications. Trajectories 40−85 s long containing 2000−3500 transitions each were calculated for tether stiffness k of 0.3, 0.6, and 1 pN/nm (Figure 2B) as well as for a simulation with the force applied directly to the end of the molecule (no bead or tether). In each case, the trajectories were analyzed as done for the experimental data, obtaining $P(x)$ (Figure 2C), $P(x|\mathrm{TP})$ (Figure 2D), and $p(\mathrm{TP}|x)$ (Figure 2E).

Although $P(x|\mathrm{TP})$ has similar features for all four simulations, as might be expected because $P(x|\mathrm{TP})$ depends primarily on the properties of the folding landscape and should be minimally affected by the tether compliance, $P(x)$ has significantly more weight between x_1 and x_2 at lower stiffness values because of the additional fluctuations caused by the increased tether compliance. As a result, whereas $p(\mathrm{TP}|x)$ is highly peaked around $x^‡$ (Figure 2E, dashed line) when there is no tether, reaching close to the expected value of 1/2 (Figure 2E, top panel), the amplitude of this peak is suppressed as tether compliance is increased, with the effect increasing as k decreases(Figure 2E, bottom three panels). Because these simulations involved purely 1D diffusive motion, for comparison we calculated $\Phi(x) = 2p_{\mathrm{fold}}(x)[1 - p_{\mathrm{fold}}(x)]$ from the simulated trajectories (Figure 2E, orange). Notably, $p(\mathrm{TP}|x)$ agrees well with $\Phi(x)$ for the simulation without tether and is not bad for the high-k simulation, but the agreement is not very good for the lower-k simulations, indicating that the tether compliance can indeed have a significant effect.

Because the instrumental compliance affects $p(\mathrm{TP}|x)$ primarily by adding extra statistical weight to $P(x)$ in the transition region, owing to the additional fluctuations of the tether/bead system, it should be possible to correct for the compliance effects by using the "intrinsic" molecular extension distribution, $P_i(x)$, that would be expected in the absence of such extra fluctuations. To demonstrate that this is indeed the case, we calculated $P_i(x)$ for the simulated trajectories directly from the folding landscape imposed in the simulation (Figure 2A, inset) based on Boltzmann statistics and used it to replace $P(x)$ in eq 1; $p(\mathrm{TP}|x)$ was also renormalized after this substitution. (See the SI.) The resulting corrected transition-path probability was indeed highly peaked around $x^‡$ for all values of k, agreeing reasonably well with $\Phi(x)$, as expected for purely diffusive 1D motion (Figure 2F).

Having established how to account for instrumental effects in the analysis, we applied the correction for compliance effects to the experimental data, calculating $P_i(x)$ (Figure 3A, black) by empirical deconvolution of the equilibrium extension distribution (Figure 3A, gray), as described previously.[27] After

DOI: 10.1021/acs.jpclett.5b00176
J. Phys. Chem. Lett. 2015, 6, 1005−1010

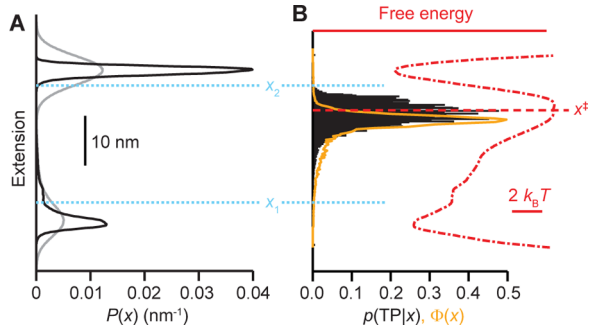

Figure 3. Compliance-corrected transition-path analysis of DNA hairpin trajectories. (A) The effects of the instrumental compliance are deconvolved from the measured equilibrium distribution (gray) to obtain the "intrinsic" distribution (black). Dotted lines: boundaries defining transition paths. (B) p(TP|x) (black) matches $\Phi(x)$ (orange) well, peaking at ∼0.45 near $x^‡$ (dashed line), as determined from the deconvolved energy landscape (dotted-dashed line).

correction, p(TP|x) reaches a maximum of ∼0.45 (Figure 3B, black), close to the expected maximum of 0.5, at an extension that is close to $x^‡$ (Figure 3B, dashed line) as found from the deconvolved energy landscape (Figure 3B, dotted-dashed line). Calculating $p_{fold}(x)$ from the trajectory via eq S1 (SI), p(TP|x) is also seen to agree fairly well with $\Phi(x)$ (Figure 3B, orange). Molecular extension is thus validated as a good reaction coordinate for the hairpin folding.

To ensure that this result was not specific to the choice of hairpin, we repeated the analysis for measurements of another two-state hairpin with a different sequence, 20TS06/T4 (Figure 4), which has a qualitatively different landscape profile.[27] When the observed equilibrium extension distribution (Figure 4B, gray) was used for the transition-path analysis, neglecting compliance effects, p(TP|x) was found to be much too low (Figure 4C, gray) and moreover peaked a few nanometers away from $x^‡$ (Figure 4C, dashed line), as determined from the deconvolved energy landscape (Figure 4C, dotted-dashed line). However, using instead the deconvolved distribution $P_i(x)$ (Figure 4B, black) to calculate p(TP|x) (Figure 4C, black), the transition-path probability agreed quite well with $\Phi(x)$ (Figure 4C, orange), peaking near 0.5 close to $x^‡$, as would be expected

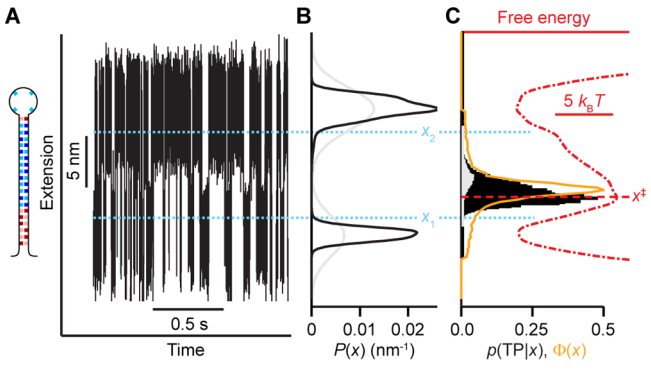

Figure 4. Transition-path analysis of hairpin with different sequence. (A) Trajectory of hairpin 20TS06/T4 extension. Inset: hairpin sequence. (B) Equilibrium extension distribution before (gray) and after (black) compliance deconvolution. (C) p(TP|x) calculated before deconvolution (gray) is too small; after deconvolution (black) it matches $\Phi(x)$ (orange) well, peaking at 0.5 near $x^‡$ (dashed line), as found from the deconvolved landscape (dotted-dashed line).

for a good reaction coordinate. Both hairpins thus demonstrate close to ideal 1D diffusive behavior.

Methods for testing reaction-coordinate quality such as transition-path and committor analyses have been applied primarily to simulations, even though experiments would benefit significantly from knowing whether the recorded observable represents a good reaction coordinate. As a result, the considerations involved in applying these methods to experiments have been minimally explored. Our work underlines that it is essential to consider how the experimental apparatus affects the measurement when assessing the quality of the reaction coordinate because tests such as the transition-path probability are sensitive to features of the measurement, such as experimental noise, that should not intrinsically have any bearing on the question of reaction-coordinate quality.

Intuitively, a good reaction coordinate is one where the projection of the full landscape results in folded and unfolded states that are well separated in x, such that $x^‡$ is occupied only along the transition paths; in contrast, projection onto a bad reaction coordinate results in overlap of the states, such that the state at $x^‡$ (folded, unfolded, or transition path) is uncertain. Adding experimental "noise" to the trajectory, however, may cause states that are intrinsically well-separated to overlap. Even though such overlap makes the reaction coordinate appear to be bad, the noise has clearly not changed the nature of the projection onto the reaction coordinate nor thus the true quality of the reaction coordinate. Only by measuring the noise added by the instrument and removing its effects does one get an accurate view of the reaction-coordinate quality. Although we have illustrated this issue with SMFS measurements, these considerations are not limited to such measurements but should apply quite generally.

Turning to the outcome of our analysis of DNA hairpin folding, the excellent agreement found between p(TP|x) and $\Phi(x)$ after accounting for instrumental effects represents a quite remarkable result: the folding dynamics of these hairpins are quantitatively what one would expect for ideal diffusion in 1D. There are reasons to believe that low-dimensional descriptions of folding can be appropriate,[39,40] and the zippering mechanism expected within single duplexes is especially simple compared with more complex tertiary structures and thus amenable to such an approach. Nevertheless, loop formation, a key step in forming the transition state for hairpin folding,[36] is not obviously a 1D process, given the many degrees of freedom involved in aligning the backbone torsional angles to bring the first few bases in the stem into contact to form basepairs. It is thus somewhat surprising that the folding matches ideal diffusion in 1D as well as it does. Previous work showing that the kinetics of hairpin folding measured under tension fit well to 1D diffusive models[41,42] supports the notion that hairpin folding is well-described as 1D, but our transition-path results represent a more direct demonstration of ideal 1D diffusive behavior.

A crucial question for future work is whether this 1D behavior extends to more complex molecules than DNA hairpins, which are a particularly simple model system for studying folding. Transition-path analysis could be applied just as well to SMFS measurements of the folding of proteins with complex tertiary structure,[17,43,44] and it will be instructive to see if these are equally well-described by 1D diffusion. The same kind of analysis could also be adapted to other assays of folding, such as fluorescence spectroscopy, to probe whether the assay geometry (e.g., imposition of a favored axis via an applied force

DOI: 10.1021/acs.jpclett.5b00176
J. Phys. Chem. Lett. 2015, 6, 1005−1010

or choice of dye location) affects the result. Experimental applications of transition-path analysis can thus help determine whether 1D diffusion really is universal in folding transitions, a question with profound implications for understanding the folding problem.

It is important that the trajectories be sampled sufficiently rapidly to acquire enough data along the transition paths for meaningful statistics to apply transition-path analysis effectively to experiments. The effects of the instrument on the measurement should be understood well enough to allow them to be accounted for in the analysis (as here, with deconvolution of compliance effects). Ideally, measurements should also be made passively in equilibrium to avoid artifactual dynamics that may result from such sources as active feedback loops.[45] Because these requirements are not overly restrictive, we expect this type of analysis to become a powerful tool for informing interpretation not only of folding measurements (e.g., from choosing the best location for applying force to a molecule[21,22,44] to comparing results from different assays) but also of other types of reactions.

■ ASSOCIATED CONTENT

Supporting Information

Sample preparation and measurements, transition path and committor analyses, folding simulations, and Figure S1. This material is available free of charge via the Internet at http://pubs.acs.org.

■ AUTHOR INFORMATION

Corresponding Author

*E-mail: michael.woodside@ualberta.ca.

Notes

The authors declare no competing financial interest.

■ ACKNOWLEDGMENTS

This work was supported by the Natural Sciences and Engineering Research Council of Canada, Alberta Prion Research Institute, and Alberta Innovates Technology Futures.

■ REFERENCES

(1) Truhlar, D. G.; Garrett, B. C.; Klippenstein, S. J. Current Status of Transition-State Theory. *J. Phys. Chem.* **1996**, *100*, 12771−12800.

(2) Hanggi, P.; Talkner, P.; Borkovec, M. Reaction-Rate Theory - 50 Years After Kramers. *Rev. Mod. Phys.* **1990**, *62*, 251−341.

(3) Hummer, G.; Kevrekidis, I. G. Coarse Molecular Dynamics of a Peptide Fragment: Free Energy, Kinetics, and Long-Time Dynamics Computations. *J. Chem. Phys.* **2003**, *118*, 10762−10773.

(4) Plotkin, S. S.; Wolynes, P. G. Non-Markovian Configurational Diffusion and Reaction Coordinates for Protein Folding. *Phys. Rev. Lett.* **1998**, *80*, 5015−5018.

(5) Makarov, D. E. Interplay of Non-Markov and Internal Friction Effects in the Barrier Crossing Kinetics of Biopolymers: Insights from an Analytically Solvable Model. *J. Chem. Phys.* **2013**, *138*, 014102.

(6) Best, R. B.; Hummer, G. Reaction Coordinates and Rates from Transition Paths. *Proc. Natl. Acad. Sci. U. S. A.* **2005**, *102*, 6732−6737.

(7) Best, R. B.; Hummer, G. Coordinate-Dependent Diffusion in Protein Folding. *Proc. Natl. Acad. Sci. U. S. A.* **2010**, *107*, 1088−1093.

(8) Bryngelson, J. D.; Wolynes, P. G. Spin Glasses and the Statistical Mechanics of Protein Folding. *Proc. Natl. Acad. Sci. U. S. A.* **1987**, *84*, 7524−7528.

(9) Dill, K. A.; MacCallum, J. L. The Protein-Folding Problem, 50 Years on. *Science* **2012**, *338*, 1042−1046.

(10) Oliveberg, M.; Wolynes, P. G. The Experimental Survey of Protein-Folding Energy Landscapes. *Q. Rev. Biophys.* **2005**, *38*, 245−288.

(11) Socci, N. D.; Onuchic, J. N.; Wolynes, P. G. Diffusive Dynamics of the Reaction Coordinate for Protein Folding Funnels. *J. Chem. Phys.* **1996**, *104*, 5860−5868.

(12) Klimov, D. K.; Thirumalai, D. Viscosity Dependence of the Folding Rates of Proteins. *Phys. Rev. Lett.* **1997**, *79*, 317−320.

(13) Dudko, O. K.; Hummer, G.; Szabo, A. Theory, Analysis, and Interpretation of Single-Molecule Force Spectroscopy Experiments. *Proc. Natl. Acad. Sci. U. S. A.* **2008**, *105*, 15755−15760.

(14) Best, R. B.; Hummer, G. Diffusion Models of Protein Folding. *Phys. Chem. Chem. Phys.* **2011**, *13*, 16902−16911.

(15) Ansari, A.; Jones, C. M.; Henry, E. R.; Hofrichter, J.; Eaton, W. A. The Role of Solvent Viscosity in the Dynamics of Protein Conformational Changes. *Science* **1992**, *256*, 1796−1798.

(16) Kubelka, J.; Henry, E. R.; Cellmer, T.; Hofrichter, J.; Eaton, W. A. Chemical, Physical, and Theoretical Kinetics of an Ultrafast Folding Protein. *Proc. Natl. Acad. Sci. U. S. A.* **2008**, *105*, 18655−18662.

(17) Yu, H.; Gupta, A. N.; Liu, X.; Neupane, K.; Brigley, A. M.; Sosova, I.; Woodside, M. T. Energy Landscape Analysis of Native Folding of the Prion Protein Yields the Diffusion Constant, Transition Path Time, and Rates. *Proc. Natl. Acad. Sci. U. S. A.* **2012**, *109*, 14452−14457.

(18) Borgia, A.; Wensley, B. G.; Soranno, A.; Nettels, D.; Borgia, M. B.; Hoffmann, A.; Pfeil, S. H.; Lipman, E. A.; Clarke, J.; Schuler, B. Localizing Internal Friction along the Reaction Coordinate of Protein Folding by Combining Ensemble and Single-Molecule Fluorescence Spectroscopy. *Nat. Commun.* **2012**, *3*, 1195.

(19) Chung, H. S.; Eaton, W. A. Single-Molecule Fluorescence Probes Dynamics of Barrier Crossing. *Nature* **2013**, *502*, 685−688.

(20) Suzuki, Y.; Dudko, O. K. Single-Molecule Rupture Dynamics on Multidimensional Landscapes. *Phys. Rev. Lett.* **2010**, *104*, 048101.

(21) Dudko, O. K.; Graham, T. G. W.; Best, R. B. Locating the Barrier for Folding of Single Molecules under an External Force. *Phys. Rev. Lett.* **2011**, *107*, 208301.

(22) Best, R. B.; Paci, E.; Hummer, G.; Dudko, O. K. Pulling Direction as a Reaction Coordinate for the Mechanical Unfolding of Single Molecules. *J. Phys. Chem. B* **2008**, *112*, 5968−5976.

(23) Du, R.; Pande, V. S.; Grosberg, A. Y.; Tanaka, T.; Shakhnovich, E. S. On the Transition Coordinate for Protein Folding. *J. Chem. Phys.* **1998**, *108*, 334−350.

(24) Rohrdanz, M. A.; Zheng, W.; Clementi, C. Discovering Mountain Passes via Torchlight: Methods for the Definition of Reaction Coordinates and Pathways in Complex Macromolecular Reactions. *Annu. Rev. Phys. Chem.* **2013**, *64*, 295−316.

(25) Bolhuis, P. G.; Chandler, D.; Dellago, C.; Geissler, P. L. Transition path sampling: Throwing Ropes Over Rough Mountain Passes, in the Dark. *Annu. Rev. Phys. Chem.* **2002**, *53*, 291−318.

(26) Morrison, G.; Hyeon, C.; Hinczewski, M.; Thirumalai, D. Compaction and Tensile Forces Determine the Accuracy of Folding Landscape Parameters from Single Molecule Pulling Experiments. *Phys. Rev. Lett.* **2011**, *106*, 138102.

(27) Woodside, M. T.; Anthony, P. C.; Behnke-Parks, W. M.; Larizadeh, K.; Herschlag, D.; Block, S. M. Direct Measurement of the Full, Sequence-Dependent Folding Landscape of a Nucleic Acid. *Science* **2006**, *314*, 1001−1004.

(28) Gebhardt, J. C. M.; Bornschloegla, T.; Rief, M. Full Distance-Resolved Folding Energy Landscape of One Single Protein Molecule. *Proc. Natl. Acad. Sci. U. S. A.* **2010**, *107*, 2013−2018.

(29) Chodera, J. D.; Pande, V. S. Splitting Probabilities as a Test of Reaction Coordinate Choice in Single-Molecule Experiments. *Phys. Rev. Lett.* **2011**, *107*, 098102.

(30) Chahine, J.; Oliveira, R. J.; Leite, V. B. P.; Wang, J. Configuration-Dependent Diffusion Can Shift the Kinetic Transition State and Barrier Height of Protein Folding. *Proc. Natl. Acad. Sci. U. S. A.* **2007**, *104*, 14646−14651.

DOI: 10.1021/acs.jpclett.5b00176
J. Phys. Chem. Lett. 2015, 6, 1005−1010

(31) Cellmer, T.; Henry, E. R.; Hofrichter, J.; Eaton, W. A. Measuring Internal Friction of an Ultrafast-Folding Protein. *Proc. Natl. Acad. Sci. U. S. A.* **2008**, *105*, 18320−18325.
(32) Hummer, G. From Transition Paths to Transition States and Rate Coefficients. *J. Chem. Phys.* **2004**, *120*, 516−523.
(33) Woodside, M. T.; Garcia-Garcia, C.; Block, S. M. Folding and Unfolding Single RNA Molecules under Tension. *Curr. Opin. Chem. Biol.* **2008**, *12*, 640−646.
(34) Zoldak, G.; Rief, M. Force as a Single Molecule Probe of Multidimensional Protein Energy Landscapes. *Curr. Opin. Struct. Biol.* **2013**, *23*, 48−57.
(35) Woodside, M. T.; Block, S. M. Reconstructing Folding Energy Landscapes by Single-Molecule Force Spectroscopy. *Annu. Rev. Biophys.* **2014**, *43*, 19−39.
(36) Woodside, M. T.; Behnke-Parks, W. M.; Larizadeh, K.; Travers, K.; Herschlag, D.; Block, S. M. Nanomechanical Measurements of the Sequence-Dependent Folding Landscapes of Single Nucleic Acid Hairpins. *Proc. Natl. Acad. Sci. U. S. A.* **2006**, *103*, 6190−6195.
(37) Greenleaf, W. J.; Woodside, M. T.; Abbondanzieri, E. A.; Block, S. M. Passive All-Optical Force Clamp for High-Resolution Laser Trapping. *Phys. Rev. Lett.* **2005**, *95*, 208102.
(38) Woodside, M. T.; Lambert, J.; Beach, K. S. D. Determining Intrachain Diffusion Coefficients for Biopolymer Dynamics from Single-Molecule Force Spectroscopy Measurements. *Biophys. J.* **2014**, *107*, 1647−1653.
(39) Das, P.; Moll, M.; Stamati, H.; Kavraki, L. E.; Clementi, C. Low-Dimensional, Free-Energy Landscapes of Protein-Folding Reactions by Nonlinear Dimensionality Reduction. *Proc. Natl. Acad. Sci. U. S. A.* **2006**, *103*, 9885−9890.
(40) Berezhkovskii, A.; Szabo, A. Time Scale Separation Leads to Position-Dependent Diffusion along a Slow Coordinate. *J. Chem. Phys.* **2011**, *135*, 074108.
(41) Cocco, S.; Marko, J. F.; Monasson, R. Slow Nucleic Acid Unzipping Kinetics from Sequence-Defined Barriers. *Eur. Phys. J. E: Soft Matter Biol. Phys.* **2003**, *10*, 153−161.
(42) Manosas, M.; Collin, D.; Ritort, F. Force-Dependent Fragility in RNA Hairpins. *Phys. Rev. Lett.* **2006**, *96*, 218301.
(43) Stigler, J.; Ziegler, F.; Gieseke, A.; Gebhardt, J. C. M.; Rief, M. The Complex Folding Network of Single Calmodulin Molecules. *Science* **2011**, *334*, 512−516.
(44) Jagannathan, B.; Elms, P. J.; Bustamante, C.; Marqusee, S. Direct Observation of a Force-Induced Switch in the Anisotropic Mechanical Unfolding Pathway of a Protein. *Proc. Natl. Acad. Sci. U. S. A.* **2012**, *109*, 17820−17825.
(45) Elms, P. J.; Chodera, J. D.; Bustamante, C. J.; Marqusee, S. Limitations of Constant-Force-Feedback Experiments. *Biophys. J.* **2012**, *103*, 1490−1499.

DOI: 10.1021/acs.jpclett.5b00176
J. Phys. Chem. Lett. 2015, 6, 1005−1010